Large-Scale Growth and Characterizations of Nitrogen-Doped Monolayer Graphene Sheets

Zhong Jin,[†,§] Jun Yao,[‡] Carter Kittrell,[§] and James M. Tour[†,§,⊥,*]

[†]Department of Chemistry, [‡]Applied Physics Program through the Department of Bioengineering, [§]The Smalley Institute for Nanoscale Science and Technology, and [⊥]Department of Mechanical Engineering and Materials Science, Rice University, MS-222, 6100 Main Street, Houston, Texas 77005, United States

ABSTRACT In-plane heteroatom substitution of graphene is a promising strategy to modify its properties. Doping with electron-donor nitrogen heteroatoms can modulate the electronic properties of graphene to produce an n-type semiconductor. Here we demonstrate the growth of monolayer nitrogen-doped graphene in centimeter-scale sheets using a chemical vapor deposition process with pyridine as the sole source of both carbon and nitrogen. High-resolution transmission microscopy and Raman mapping characterizations indicate that the nitrogen-doped graphene sheets are uniformly monolayered. The existence of nitrogen-atom substitution in the graphene planes was confirmed by X-ray photoelectron spectroscopy. Electrical measurements show that the nitrogen-doped graphene exhibits an n-type behavior, different from pristine graphene. The preparation of large-area nitrogen-doped graphene provides a viable route to modify the properties of monolayer graphene and promote its applications in electronic devices.

KEYWORDS: graphene · chemical vapor deposition · nitrogen-doping · n-type semiconductor

Graphene, as the two-dimensional monolayer form of sp^2-hybridized carbon, has attracted wide-ranging interest due to its promising applications in electronic devices[1] and composite materials.[2] From the perspective of practical graphene-based integrated devices,[3,4] it is important to prepare large-area graphene sheets with high-quality[5] while controlling its electrical properties.[6] The electron acceptor/donor doping of graphene is a viable approach to tailor its physical and chemical properties. For example, the field-effect behavior of graphene devices can be changed significantly by covalent edge-doping[7] and trace molecular gas adsorption.[8] Theoretical predictions show that the in-plane substitution of nitrogen heteroatoms can modulate the electronic properties of graphene to an n-type semiconductor; the resulting electron and hole transport features are asymmetric relative to the Dirac point.[9] Recently, bilayer and few-layer nitrogen-doped graphene has been synthesized by the arc charge method,[10] the chemical vapor deposition (CVD) in the presence of ammonia,[11,12] or the segregation of trace amount of carbon and nitrogen in bulk metals;[13] however, it is still a challenge to prepare large-area nitrogen-doped graphene sheets with a uniform monolayer. In this paper, we report the growth of large-area monolayer nitrogen-doped graphene sheets using a chemical vapor deposition (CVD) process with pyridine as both the sole carbon and nitrogen sources.

RESULTS AND DISCUSSION

In the present article, copper foils were used as the substrates because copper has been proven to suppress the production of precipitated carbon, leading to predominately monolayer graphene.[5] Bilayer and few-layer graphene also can be obtained on copper foils with different experimental parameters,[5] which indicate that control of the rate of feeding and deposition of the carbon source is a key factor to adjust the layer number and thickness of graphene prepared by CVD. For preparing nitrogen-doped monolayer graphene, pyridine as a nitrogen-containing small heterocycle with sp^2-hybrized C—N bonds was used as both carbon and nitrogen source. The feeding rate of pyridine was precisely controlled by Ar gas bubbling to introduce controlled amounts of carbon and nitrogen into the furnace system. Such control is essential for the production of monolayer nitrogen-doped graphene over the growth of thicker multilayer nitrogen-doped graphene.

HRTEM studies were carried out on a JEOL 2100F field emission gun transmission electron microscope; the nitrogen-doped graphene sheets had been transferred to c-flat carbon TEM grids. As shown in Figure 1a, the HRTEM image reveals the monolayer planar structure in the nitrogen-doped graphene samples, which indicates that the as-obtained graphene sheets grown on the surface of copper foils are monolayer graphene. To determine the crystallinity of the graphene sheets, a selected-area electron diffraction (SAED) pattern was also

* Address correspondence to tour@rice.edu.

Received for review February 24, 2011 and accepted April 8, 2011.

Published online April 08, 2011
10.1021/nn200766e

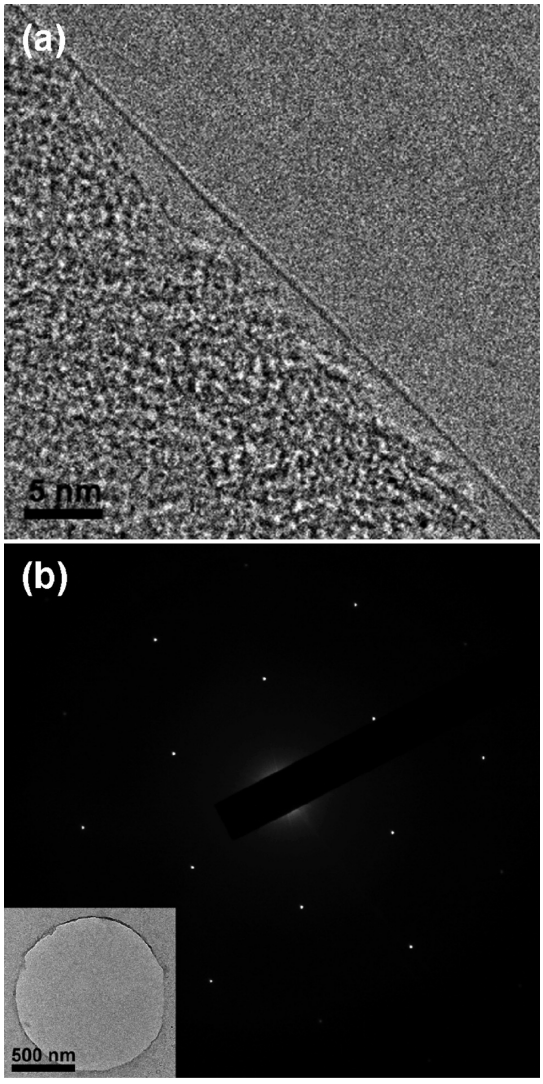

Figure 1. (a) HRTEM image of a monolayer nitrogen-doped graphene sheet. (b) SAED pattern of nitrogen-doped graphene. The inset shows a low-resolution TEM image of the nitrogen-doped graphene suspended above a vacant microhole (with a diameter of ~1 μm) of a c-flat carbon TEM grid, from which the SAED pattern was collected.

taken by using selected-area apertures from the graphene sheet suspended onto a vacant micrometer-sized hole on a c-flat carbon TEM grid. Figure 1b shows the SAED pattern where only one set of hexagonal diffraction spots was detected, which indicates that the suspended graphene sheet is a single crystalline domain within the selected area.[14] The SAED characterization implies that in spite of the nitrogen-heteroatom incorporation in the hexagonal carbon network, the graphene sheets are well-ordered crystalline structures, which is similar to the previous results for few-layer nitrogen-doped graphene.[12] As shown in Figure 2a, an area near the edge of a nitrogen-doped graphene sheet was observed *via* an optical microscope. The AFM image (Figure 2b) collected at the same area shows the height of this graphene flake measured from a line profile is about 1.0−1.2 nm. Some wrinkles and roughness can also be

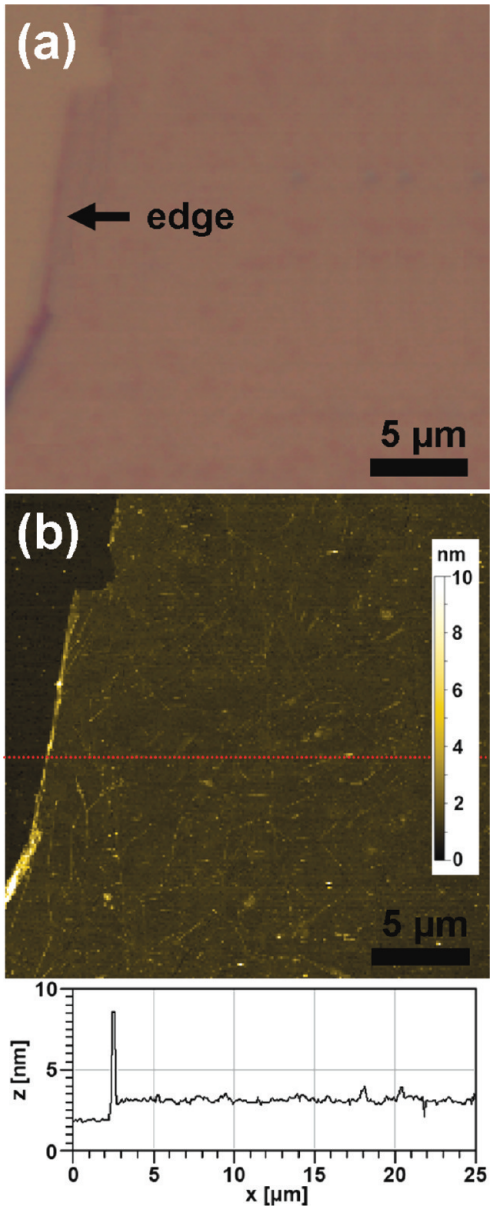

Figure 2. (a) Optical image and (b) AFM image of the same area of a monolayer nitrogen-doped graphene sheet. A height profile was taken from the red dashed line, which shows the height of the graphene flake is about 1.0−1.2 nm.

found on the graphene sheet with AFM characterization, which may due to the transfer process or the grain boundaries of the graphene domains.[15,16]

To further evaluate the structure of nitrogen-doped graphene sheets, Raman spectra were taken on a Renishaw 1000 Raman spectroscope with the laser at 514.5 nm excitation wavelength. A typical Raman spectrum of the nitrogen-doped graphene is displayed in Figure 3a. Three main peaks are assigned in the Raman spectrum: the D band (~1345 cm^{-1}), G band (~1585 cm^{-1}) and 2D band (~2684 cm^{-1}). The G band shows a blue-shift compared to that from pristine monolayer graphene,[17] which is a sign of atomic insertions.[18−20] The D band is accompanied by a D* band at ~1624 cm^{-1},

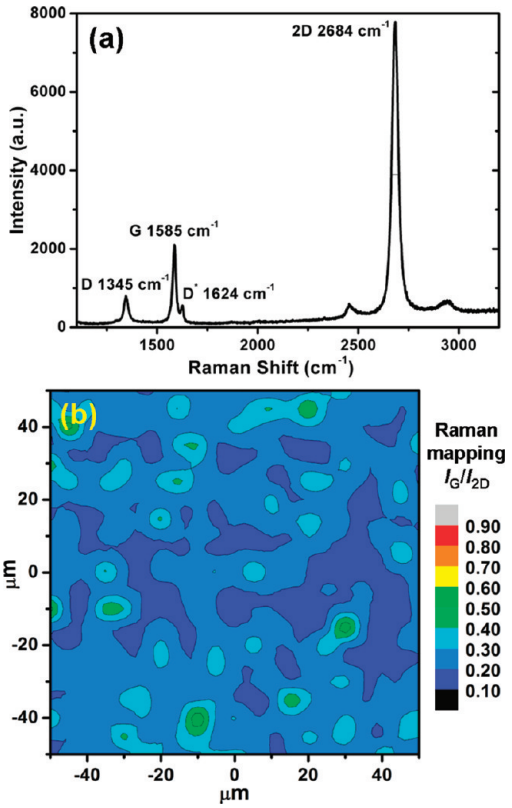

Figure 3. (a) Typical Raman spectrum of nitrogen-doped monolayer graphene sheets transferred onto SiO_2/Si substrates; the laser excitation wavelength was 514.5 nm. (b) Raman mapping of large-area nitrogen-doped graphene film. The color gradations represent the value of I_G/I_{2D}, which is the intensity ratio of the G band to the 2D band of the Raman spectrum collected at the same position. The Raman mapping signals were taken from a 100 × 100 μm^2 area of the nitrogen-doped graphene transferred onto SiO_2/Si substrate.

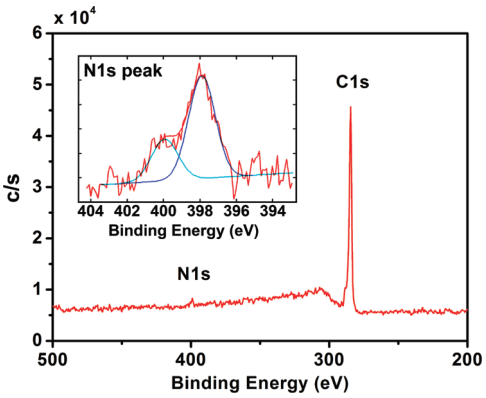

Figure 4. XPS spectrum of nitrogen-doped graphene. The corresponding inset shows the high-resolution scan of nitrogen N1s peak; the N1s signal is split at 397.9 and 400.0 eV.

which was also observed in the Raman spectra of few-layer nitrogen-doped graphene.[10] The intensity ratio of D band and G band I_D/I_G reveals the in-plane crystallite dimension and the degree of in-plane defects and edge defects in the carbon materials. Normally the I_D/I_G is about 0.3−0.4, which is indicative of the atomic insertions, or doping of the graphene sheets, as the nitrogen insertions in the sp^2 carbon matrices introduce topological defects.[18] The shape of the 2D band is sensitive to the number of graphene layers.[21] In this spectrum the 2D peak is a sharp peak with full-width at half-maximum (fwhm) of ~35 cm^{-1}, corresponding to monolayer graphene, as bilayer and few-layer graphene have broader and blue-shifted 2D bands when compared to the monolayer graphene.[21,22] Another key factor in verification of monolayer graphene is the intensity ratio of the G band to the 2D band, I_G/I_{2D}.[23] The I_G/I_{2D} in this specific Raman spectrum is ~0.27, confirming the monolayered structure. To further investigate the homogeneity of the nitrogen-doped graphene, large-area Raman mapping within a 100 × 100 μm^2 area was performed, as shown in Figure 3b. The value of I_G/I_{2D} across the graphene surface is shown as color gradations, which represent the Raman intensity ratios of the G band and the 2D band at the same position. From the Raman map, it is evident that $0.1 < I_G/I_{2D} < 0.6$, usually between 0.2 and 0.4. On the basis of the Raman and HRTEM characterization, we can conclude that the as-obtained nitrogen-doped graphene is monolayer.

To investigate the content of nitrogen atoms, XPS was performed on the nitrogen-doped graphene with a PHI Quantera SXM scanning X-ray microprobe. In the survey scan of XPS, the peaks at 284.5 and 398.3 eV correspond to C1s peak of sp^2 carbon and N1s peak of the doped nitrogen, respectively. In the high resolution scan (the inset of Figure 4), the asymmetric N1s peak can be divided into two components, indicating that nitrogen atoms are in two different binding states inserted into the graphene network, comparable to nitrogen-doped carbon nanotubes.[10,24] The peak at 397.9 eV corresponds to "pyridinic" nitrogen.[10] The peak at 400.0 eV is due to quaternary nitrogen in the graphene sheets, which corresponds to the highly coordinated nitrogen atoms that replaced carbon atoms within the graphene sheets.[10] The N1s signal of nitrogen-doped graphene in this work is different from the melamine-PMMA derived nitrogen-doped graphene that only shows one quaternary nitrogen peak,[25] which is indicative of the different doping states of nitrogen atoms in these two materials. The area ratio of the pyridinic nitrogen peak and quaternary nitrogen peak is 2.5:1. The peak for pyridinic nitrogen is higher, which indicates the nitrogen atoms doped in the graphene lattice are mainly in the form of pyridinic nitrogen. The pyridinic nitrogen atoms are responsible for introducing donor states close to the Fermi level.[24] Calculated from XPS data, the atomic percentage of nitrogen in the as-obtained nitrogen-doped graphene was found to be ~2.4%. The XPS results along with the changes in the G band and the other bands in the Raman spectra mentioned earlier suggest that the dopant nitrogen heteroatoms have been substituted for carbon atoms in the graphene lattice.

We performed electrical characterizations on both nitrogen-doped graphene and pristine graphene grown

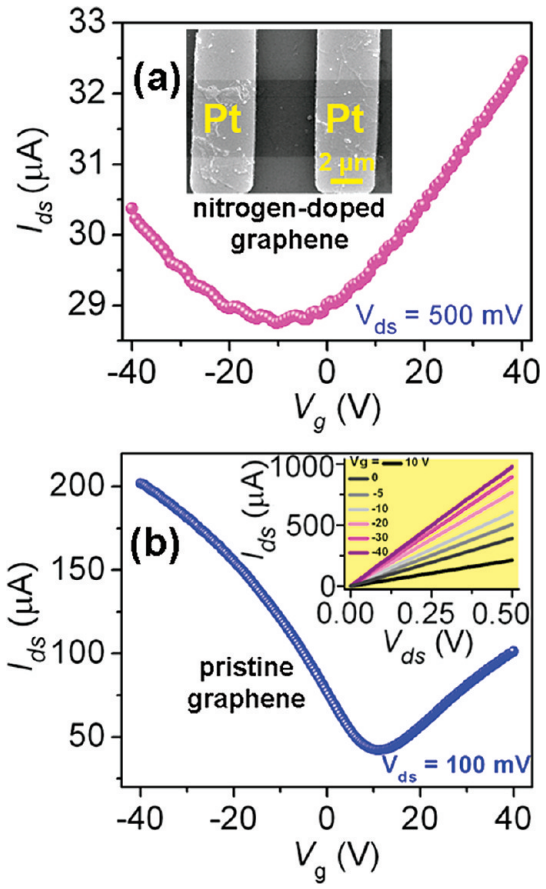

Figure 5. Transport properties in nitrogen-doped and pristine graphene devices. (a) Source-drain current (I_{ds}) with respect to the backgate voltage (V_g) of a nitrogen-doped graphene device, with the neutrality point at −10 V. The estimated carrier mobility is ~5 cm^2 V^{-1} s^{-1}. The inset shows a top-view SEM image of the actual graphene device. (b) I_{ds}−V_g relationship from a typical pristine graphene device having similar dimensions as shown in panel a. The calculated carrier mobility in this particular device is ~2000 cm^2 V^{-1} s^{-1}. The top-right inset shows a linear current−voltage (I_{ds}−V_{ds}) relationship in the pristine graphene device at different back gate voltages.

with CH_4 and H_2. The graphenes were transferred to a highly doped silicon substrate (ρ = 0.005 Ω·cm) capped with 200-nm-thick thermally grown SiO_2. Then oxygen-plasma etching was used to define graphene stripes, after which electron-beam lithography and lift-off methods were employed to pattern Pt electrodes (30-nm-thick with a 5 nm Ti adhesion layer). The inset in Figure 5a shows a scanning electron microscopy (SEM) image of an as-made device. The devices with nitrogen-doped graphene strips show an apparent shift of the neutrality point toward the negative gate voltage region. Figure 5a shows the transport behavior in a typical nitrogen-doped graphene device with the neutrality point at −10 V. The highly doped silicon substrate was used as a back-gate electrode. Electrical measurements were performed under vacuum (~10^{-5} Torr) in a probe station using an Agilent 4155C semiconductor parameter analyzer. The devices were kept in the vacuum chamber over 7 days before electrical characterization.[26,27] A SEM image of nitrogen-doped graphene with Ti/Pt electrodes but without oxygen-plasma etching is also shown in Figure S1 (Supporting Information), indicating that the large-area nitrogen-doped graphene sheets transferred on SiO_2/Si chips are continuous.

Besides the shift of the neutrality point, both the conductance and ON/OFF ratio decrease compared to those in pristine graphene devices. As a result, the estimated mobility in these nitrogen-doped graphene devices is reduced to ~5 cm^2 V^{-1} s^{-1}, about 2 orders of magnitude lower than in pristine graphene devices. The measured carrier mobility of nitrogen-doped graphene in this present article is comparable to the results obtained by other methods.[25] The reduction in carrier mobility is expected as both pyridinic nitrogen and substituting nitrogen in the graphene lattice introduce additional scattering centers. The electrical phenomena of n-type behavior in nitrogen-doped graphene are reproducible (more than 20 devices were made and characterized), with the largest voltage shift over −30 V toward the negative gate voltage region (see Supporting Information Figure S2) and a standard deviation of ~6 V. The reproducibility excludes extrinsic effects such as physisorption[26] or charge trapping[28] introduced during the fabrication process.

In contrast, the pristine graphene device control samples, without nitrogen doping, show typical ambipolar transport behavior (Figure 5b). The slight shift of the neutrality point to the positive gate voltage region is a result of residual adsorbants such as water, which is frequently observed.[29,30] Using a simple capacitor model,[31] the estimated carrier (hole) mobility in the pristine graphene devices is between 400 and 2000 cm^2 V^{-1} s^{-1}, which is within the typical carrier mobility range for CVD graphene.[5,32]

SUMMARY

A method was developed to prepare monolayer nitrogen-doped graphene using a CVD process where pyridine acts as both the sole carbon and the nitrogen sources. Analysis by HRTEM, Raman spectroscopy, and XPS established that the process resulted in in-plane nitrogen-substitution in the monolayer graphene. The doping was confirmed by further electrical measurements of the nitrogen-doped graphene, which clearly shows n-type transport behavior.

METHODS

Typically, a ~4 cm^2 copper foil (Sigma-Aldrich, 25 μm thick, 99.999% purity) was placed at the center of a fused quartz tube furnace (Lindberg/Blue M, fused quartz tube inner diameter 22 mm). The furnace tube was evacuated and then heated to 1000 °C under a 400 sccm H_2 flow with a H_2 gas pressure of ~6 Torr. After

annealing for 20 min under those conditions, pyridine vapor was introduced into the reactor by passing a 40 sccm Ar gas flow through a bubbler containing liquid pyridine. The temperature and gas flows were maintained in the furnace tube for 10 min with a total pressure of ~7 Torr. After the growth period, the Ar gas flow was stopped and the sample was cooled to room temperature under H_2 gas flow. We also prepared pristine graphenes as control samples using a similar CVD process with methane as the carbon source. Instead of pyridine vapor carried by Ar gas flow, 40 sccm of methane was introduced to the furnace tube together with H_2 gas during the growth period. Other experimental conditions were the same as for the growth of nitrogen-doped graphene sheets.

After the growth process, the almost transparent, large-area graphene sheets were transferred from the copper foils to other substrates such as SiO_2/Si chips or glass slides, for further characterization and electronic measurements. Normally, a poly(methyl methacrylate) (PMMA) film was spin-coated onto the surface of the copper foil-grown graphene film. Then the PMMA/graphene layer was separated from the copper foil by etching in a 1 M $CuCl_2$/6 M HCl aqueous solution and then the PMMA/graphene film was placed on the surface of deionized water to remove residual salts or water-soluble contaminants. The PMMA/graphene film was then transferred to a SiO_2/Si substrate bearing a 200-nm-thick thermally grown SiO_2 layer. After drying in a vacuum oven at 60 °C and 40 Torr, the PMMA film was dissolved and washed away by soaking the substrate in acetone overnight, thus leaving only the graphene sheets on the substrate.

Acknowledgment. Financial support was provided by the U.S. Department of Energy's Office of Energy Efficiency and Renewable Energy within the Hydrogen Sorption Center of Excellence at the National Renewable Energy Laboratory, DE-FC-36-05GO15073; the AFOSR (FA9550-09-1-0581), the AFOSR through an STTR with PrivaTran, Inc., and the ONR MURI program (No. 00006766).

Supporting Information Available: Transport properties of additional nitrogen-doped graphene devices with the largest voltage shift over −30 V toward the negative gate voltage region. This material is available free of charge *via* the Internet at http://pubs.acs.org.

REFERENCES AND NOTES

1. Novoselov, K. S.; Geim, A. K.; Morozov, S. V.; Jiang, D.; Zhang, Y.; Dubonos, S. V.; Grigorieva, I. V.; Firsov, A. A. Electric Field Effect in Atomically Thin Carbon Films. *Science* **2004,** *306*, 666–669.
2. Stankovich, S.; Dikin, D. A.; Dommett, G. H. B.; Kohlhaas, K. M.; Zimney, E. J.; Stach, E. A.; Piner, R. D.; Nguyen, S. T.; Ruoff, R. S. Graphene-Based Composite Materials. *Nature* **2006,** *442*, 282–286.
3. Geim, A. K.; Novoselov, K. S. The Rise of Graphene. *Nat. Mater.* **2007,** *6*, 183–191.
4. Lin, Y. M.; Dimitrakopoulos, C.; Jenkins, K. A.; Farmer, D. B.; Chiu, H. Y.; Grill, A.; Avouris, P. 100-Ghz Transistors from Wafer-Scale Epitaxial Graphene. *Science* **2010,** *327*, 662–662.
5. Li, X. S.; Cai, W. W.; An, J. H.; Kim, S.; Nah, J.; Yang, D. X.; Piner, R.; Velamakanni, A.; Jung, I.; Tutuc, E.; *et al.* Large-Area Synthesis of High-Quality and Uniform Graphene Films on Copper Foils. *Science* **2009,** *324*, 1312–1314.
6. Han, M. Y.; Ozyilmaz, B.; Zhang, Y. B.; Kim, P. Energy Band-Gap Engineering of Graphene Nanoribbons. *Phys. Rev. Lett.* **2007,** *98*, 206805.
7. Wang, X. R.; Li, X. L.; Zhang, L.; Yoon, Y.; Weber, P. K.; Wang, H. L.; Guo, J.; Dai, H. J. N-Doping of Graphene through Electrothermal Reactions with Ammonia. *Science* **2009,** *324*, 768–771.
8. Schedin, F.; Geim, A. K.; Morozov, S. V.; Hill, E. W.; Blake, P.; Katsnelson, M. I.; Novoselov, K. S. Detection of Individual Gas Molecules Adsorbed on Graphene. *Nat. Mater.* **2007,** *6*, 652–655.
9. Lherbier, A.; Blase, X.; Niquet, Y. M.; Triozon, F.; Roche, S. Charge Transport in Chemically Doped 2D Graphene. *Phys. Rev. Lett.* **2008,** *101*, 036808.
10. Panchokarla, L. S.; Subrahmanyam, K. S.; Saha, S. K.; Govindaraj, A.; Krishnamurthy, H. R.; Waghmare, U. V.; Rao, C. N. R. Synthesis, Structure, and Properties of Boron- and Nitrogen-Doped Graphene. *Adv. Mater.* **2009,** *21*, 4726–4730.
11. Wei, D. C.; Liu, Y. Q.; Wang, Y.; Zhang, H. L.; Huang, L. P.; Yu, G. Synthesis of N-Doped Graphene by Chemical Vapor Deposition and Its Electrical Properties. *Nano Lett.* **2009,** *9*, 1752–1758.
12. Qu, L.; Liu, Y.; Baek, J.-B.; Dai, L. Nitrogen-Doped Graphene as Efficient Metal-free Electrocatalyst for Oxygen Reduction in Fuel Cells. *ACS Nano* **2010,** *4*, 1321–1326.
13. Zhang, C.; Fu, L.; Liu, N.; Liu, M.; Wang, Y.; Liu, Z. Synthesis of Nitrogen-Doped Graphene Using Embedded Carbon and Nitrogen Sources. *Adv. Mater.* **2011,** *23*, 1020–1024.
14. Meyer, J. C.; Geim, A. K.; Katsnelson, M. I.; Novoselov, K. S.; Booth, T. J.; Roth, S. The Structure of Suspended Graphene Sheets. *Nature* **2007,** *446*, 60–63.
15. Kim, K.; Lee, Z.; Regan, W.; Kisielowski, C.; Crommie, M. F.; Zettl, A. Grain Boundary Mapping in Polycrystalline Graphene. *ACS Nano* **2011,** *5*, 2142–2146.
16. Huang, P. Y.; Ruiz-Vargas, C. S.; van der Zande, A. M.; Whitney, W. S.; Levendorf, M. P.; Kevek, J. W.; Garg, S.; Alden, J. S.; Hustedt, C. J.; Zhu, Y.; *et al.* Grains and Grain Boundaries in Single-Layer Graphene Atomic Patchwork Quilts. *Nature* **2011,** *469*, 389–392.
17. Ferrari, A. C.; Meyer, J. C.; Scardaci, V.; Casiraghi, C.; Lazzeri, M.; Mauri, F.; Piscanec, S.; Jiang, D.; Novoselov, K. S.; Roth, S.; *et al.* Raman Spectrum of Graphene and Graphene Layers. *Phys. Rev. Lett.* **2006,** *97*, 187401.
18. Ferrari, A. C. Raman Spectroscopy of Graphene and Graphite: Disorder, Electron-Phonon Coupling, Doping and Nonadiabatic Effects. *Solid State Commun.* **2007,** *143*, 47–57.
19. Das, A.; Pisana, S.; Chakraborty, B.; Piscanec, S.; Saha, S. K.; Waghmare, U. V.; Novoselov, K. S.; Krishnamurthy, H. R.; Geim, A. K.; Ferrari, A. C.; *et al.* Monitoring Dopants by Raman Scattering in an Electrochemically Top-Gated Graphene Transistor. *Nat. Nanotechnol.* **2008,** *3*, 210–215.
20. Yan, J.; Zhang, Y.; Kim, P.; Pinczuk, A. Electric Field Effect Tuning of Electron-Phonon Coupling in Graphene. *Phys. Rev. Lett.* **2007,** *98*, 166802.
21. Graf, D.; Molitor, F.; Ensslin, K.; Stampfer, C.; Jungen, A.; Hierold, C.; Wirtz, L. Spatially Resolved Raman Spectroscopy of Single- and Few-Layer Graphene. *Nano Lett.* **2007,** *7*, 238–242.
22. Gupta, A.; Chen, G.; Joshi, P.; Tadigadapa, S.; Eklund, P. C. Raman Scattering from High-Frequency Phonons in Supported N-Graphene Layer Films. *Nano Lett.* **2006,** *6*, 2667–2673.
23. Ni, Z. H.; Wang, H. M.; Kasim, J.; Fan, H. M.; Yu, T.; Wu, Y. H.; Feng, Y. P.; Shen, Z. X. Graphene Thickness Determination Using Reflection and Contrast Spectroscopy. *Nano Lett.* **2007,** *7*, 2758–2763.
24. Terrones, M.; Ajayan, P. M.; Banhart, F.; Blase, X.; Carroll, D. L.; Charlier, J. C.; Czerw, R.; Foley, B.; Grobert, N.; Kamalakaran, R.; *et al.* N-Doping and Coalescence of Carbon Nanotubes: Synthesis and Electronic Properties. *Appl. Phys. A: Mater. Sci. Process.* **2002,** *74*, 355–361.
25. Sun, Z. Z.; Yan, Z.; Yao, J.; Beitler, E.; Zhu, Y.; Tour, J. M. Growth of Graphene from Solid Carbon Sources. *Nature* **2010,** *468*, 549–552.
26. Ryu, S.; Liu, L.; Berciaud, S.; Yu, Y.-J.; Liu, H.; Kim, P.; Flynn, G. W.; Brus, L. E. Atmospheric Oxygen Binding and Hole Doping in Deformed Graphene on a SiO_2 Substrate. *Nano Lett.* **2010,** *10*, 4944–4951.
27. Yao, J.; Jin, Z.; Zhong, L.; Natelson, D.; Tour, J. M. Two-Terminal Nonvolatile Memories Based on Single-Walled Carbon Nanotubes. *ACS Nano* **2009,** *3*, 4122–4126.
28. Joshi, P.; Romero, H. E.; Neal, A. T.; Toutam, V. K.; Tadigadapa, S. A. Intrinsic Doping and Gate Hysteresis in Graphene Field Effect Devices Fabricated on SiO_2 Substrates. *J. Phys.: Condens. Matter* **2010,** *22*, 334214.

29. Chen, Z.; Lin, Y.-M.; Rooks, M. J.; Avouris, P. Graphene Nanoribbon Electronics. *Phys. E* **2007,** *40*, 228–232.
30. Han, M. Y.; Ozyilmaz, B.; Zhang, Y.; Kim, P. Energy Band-Gap Engineering of Graphene Nanoribbons. *Phys. Rev. Lett.* **2007,** *98*, 206805.
31. Bolotin, K. I.; Sikes, K. J.; Jiang, Z.; Klima, M.; Fudenberg, G.; Hone, J.; Kim, P.; Stormer, H. L. Ultrahigh Electron Mobility in Suspended Graphene. *Solid State Commun.* **2008,** *146*, 351–355.
32. Reina, A.; Jia, X.; Ho, J.; Nezich, D.; Son, H.; Bulovic, V.; Dresselhaus, M. S.; Kong, J. Large Area, Few-Layer Graphene Films on Arbitrary Substrates by Chemical Vapor Deposition. *Nano Lett.* **2008,** *9*, 30–35.